

## Localisation of Manganese Accumulated by Microalgal Cells Using Energy-Dispersive X-ray Microanalysis in the Electron Microscope

FARID ABU-SHAMMALA

Department of Chemistry, Islamic University of Gaza  
P.O. Box 108, Gaza City, Palestine Via Israel

The sites of accumulation of manganese in cells of the unicellular chlorophyte algae *Chlamydomonas* and *Chlorella*, and the blue-green alga *Anabaena*, have been determined by energy-dispersive X-ray microanalysis of freeze-dried cryosections in a scanning transmission electron microscope. Following exposure of the cells to a solution containing 200 ppm manganese for 24 h, static analyses of cellular compartments and digital X-ray mapping of element distributions in the cryosections showed that the manganese was nearly all concentrated in electron-dense granules within the cells. In *Anabaena*, however, large amounts of Mn were also found in the gelatinous sheath in which many of the blue-green cells were enveloped. Binding of manganese in the cell wall, except in the external mucilaginous layer in *Anabaena*, could not be demonstrated. The manganese concentration in the granules was highest in *Chlamydomonas* cells, averaging about 10% by weight. The intracellular bodies, presumed to be polyphosphate inclusions because of the presence of high concentrations of P and O, also contained Mg and some C. In *Chlorella* cells, these elements were accompanied by Na, S, Cl and K and in *Anabaena*, by Ca. The mean calculated O:P stoichiometry from analyses of individual granules was about 1:9:1 for *Chlorella*, and > 3:1 for *Chlamydomonas* and *Anabaena*. Measurements of the O:P ratio with time, and analyses of some cells at low temperature, suggested that observed O:P stoichiometries below 4:1 could not be explained simply by beam-induced loss of oxygen during analysis. Thus P in the granules must be present in forms other than simple phosphate, possibly as long-chain or two-dimensional polymeric polyphosphate. The deposition of manganese in intracellular granules, and the trapping of Mn in the external mucilage in the blue-green alga, appear to be mechanisms by which the algal cells can reduce toxic physiological effects of the element.

### INTRODUCTION

In the present study, energy-dispersive X-ray microanalysis in a scanning transmission electron microscope has been used to determine the localization and distribution of manganese accumulated by living microalgal cells of the two chlorophyte species *Chlamydomonas* and *Chlorella*, and of the cyanophyte alga *Anabaena*. Algal strains displaying tolerance to polluting metal in the environment have been observed<sup>1</sup>, though there is little information about the mechanism of manganese tolerance and accumulation by such microorganisms. A sound knowledge of the interaction between the metal ion and microorganisms is fundamental in understanding the behaviour and fate of metal ions in the environment. As such mechanisms of interaction become better understood, the

organisms may have a potential role in the *in situ* decontamination of metal-polluted aqueous environments.

Energy-dispersive X-ray microanalysis is a useful technique to study the binding of metal ions by microorganisms. In particular, the technique can be employed to simultaneously determine the distributions of a number of different elements in various regions of the specimen being studied. Aiking *et al.*<sup>2</sup> and Macaskie *et al.*<sup>3</sup> have used electron microscopy and X-ray microanalysis to study the location of cadmium and the nature of the cadmium binding in *Klebsiella aerogenes* and *Citrobacter* sp., while Starodub and Trevors<sup>4</sup> have studied the difference in silver accumulation between silver-resistant and sensitive strains of *Escherichia coli*. Hafeli *et al.*<sup>5</sup> and Slawson *et al.*<sup>6-8</sup> have used these techniques to investigate the distribution of silver on *Pseudomonas stutzeri* and have shown that the cells possess a silver resistance mechanism.

In this work, the sites of accumulation of manganese by the three unicellular algae have been identified by X-ray microanalysis, including X-ray elemental mapping, as part of an investigation into the mechanisms of interaction between this element and the organisms. In order to minimise loss or redistribution of the Mn due to specimen preparation for electron microscopy, microanalysis has been carried out on freeze-dried thin cryosections prepared from rapidly frozen fresh cell suspensions.

## EXPERIMENTAL

**Specimen preparation:** Algae samples of all three algae were obtained from the Botany Department of the University of Queensland. The algae were grown in a medium consisting of a standard algal culture medium made up of (AR salt used): KNO<sub>3</sub>, 1.25 g; KH<sub>2</sub>PO<sub>4</sub>, 1.25 g; MgSO<sub>4</sub>·7H<sub>2</sub>O, 1.00 g; CaCl<sub>2</sub>·2H<sub>2</sub>O, 84 mg; FeSO<sub>4</sub>·7H<sub>2</sub>O, 2 mg; H<sub>3</sub>BO<sub>3</sub>, 2.88 mg; MnCl<sub>2</sub>·4H<sub>2</sub>O, 1.81 mg; ZnSO<sub>4</sub>·7H<sub>2</sub>O, 0.22 mg; Na<sub>2</sub>MoO<sub>4</sub>·2H<sub>2</sub>O, 0.02467 mg; CoCl<sub>2</sub>·6H<sub>2</sub>O, 0.04 mg; 1 L deionised water. The cells of *Chlorella*, *Chlamydomonas* and *Anabaena* were collected from their medium by centrifugation and washed several times with deionised water and then they were suspended in a solution containing 200 ppm manganese (MnCl<sub>2</sub>·4H<sub>2</sub>O) at pH 6.0 for 24 h.

Cryofixation and cryosectioning of the algal cells in suspension was used to retain the manganese distribution in the cells as close as possible to the *in vivo* condition. The suspensions were spun down, then resuspended in 20% bovine serum albumin (BSA) + 2% agarose in distilled water. The BSA and agarose were used to provide a support matrix for the cells for cryosectioning and freeze-drying, and to promote better cryofixation of the suspension. A small drop of the suspension was placed on the tip of a small stainless steel pin, and rapidly plunge-frozen in liquid propane cooled with liquid nitrogen in a Reichert (Leica) KF80 cryofixation device. The pins were subsequently stored under liquid nitrogen prior to cryosectioning.

Frozen sections were cut with a glass knife to a nominal thickness of 300 nm at -90°C using either an RMC MT7 ultramicrotome fitted with a CR21 cryosectioning system (RMC Inc., Tucson AZ, USA), or a Leica FCS cryoultramicrotome (Leica AG, Vienna). The cryosections were collected with an eyelash probe onto Cu 100-mesh folding grids coated with a thin Formvar film, which

had been stabilised with a light coating of carbon. The sections were freeze-dried overnight at  $-80^{\circ}\text{C}$  under a vacuum of about  $10^{-5}$  Torr ( $1.3 \times 10^{-3}$  Pa), and stored in a desiccator until examination in the electron microscope.

*Electron microscopy and X-ray microanalysis:* A 200 kV Philips CM200 Transmission Electron Microscope (Philips Electron Optics, Eindhoven, the Netherlands) at the AEMF, QUT, was used for the observation and X-ray microanalysis of the algal cryosections. The instrument was equipped with a Link ISIS energy-dispersive X-ray analysis system and atmospheric thin window X-ray detector (Link Analytical, High Wycombe, UK). The cryosections were examined in Scanning Transmission (STEM) mode using both bright-field and annular dark-field imaging, the latter mode yielding better contrast because of its dependence on mass density differences in the sections. Digital STEM images were acquired using the Link microanalyser. Because of the fragility of the dried cryosections, rapid scan digital images proved superior to STEM photography, where the slow scan would frequently disrupt the sections.

X-ray microanalysis was performed by analysing small rastered areas or points in the cells for 100–200 secs with an electron probe current of about 0.5 nA. Element distributions over a defined area were determined using digital X-ray mapping (elemental imaging) at  $128 \times 128$  pixel resolution, with a total acquisition time of about 2 h. The fragile sections tended to drift under the beam during extended analysis periods, and a link utility, Beamtrack, was therefore employed to monitor and correct for specimen drift during acquisition of the X-ray maps.

The possibility of beam-induced element loss during long static analyses was examined in some experiments by sequential 10 or 15 sec analyses of the same position. As such beam effects can be markedly reduced at low temperature, the stability of the elemental ratios was checked also by analysis of some specimens at  $-160^{\circ}\text{C}$  using a Gatan 626 cryoholder (Gatan Inc., Pleasanton CA, USA).

*Calculation of element concentrations and ratios:* The elemental X-ray intensities were calculated from the X-ray spectra by a Link Analytical filtered least-squares fitting procedure. Element concentrations were determined using a thin-film quantitation package (TEMQuant), which normalises the measured elements to 100%, and requires estimates of the sample density and equivalent thickness at the analysed area for sample X-ray absorption corrections. The application of this quantitation model was feasible in this biological material since virtually all elemental constituents including carbon and oxygen (excluding only H) could be analysed. For the intracellular granules, a density of about  $2.2 \text{ g/cm}^3$  was estimated from the elemental composition, and an absorption thickness was derived from the particle dimensions. Because of the requirement for normalisation, the elemental ratios obtained by this quantitation procedure are generally more accurate than the absolute element concentrations, especially for biological materials. The measurement of carbon was problematic. Corrections were made for the carbon contribution from the thin support film, but the uncertainty in this correction, together with the possibility of C loss or gain due to etching or contamination, respectively, of the sample in the electron beam, make the carbon analyses the least reliable. The oxygen X-ray contribution from the support film was proportionately very small, and a correction for O was usually not necessary.

The sensitivity for nitrogen is poor by this analytical method, as the N X-rays are strongly absorbed by carbon in both the sample and the X-ray detector window. However, N was included in the results when it was measured at statistically significant levels.

Elemental ratios were expressed relative to phosphorus. In order to calculate the stoichiometry of O to P in the intracellular granules from their X-ray intensities, a ratio of analytical sensitivities for O and P (the O : P k-factor) is required. This factor was determined experimentally from the analysis of small particles of  $\text{KH}_2\text{PO}_4$  mounted on a thin support film<sup>9</sup>, and the measurement extrapolated to zero thickness, to eliminate X-ray absorption effects, by the method of Horita *et al.*<sup>10</sup> The stability of the phosphate group was checked by monitoring the O : P ratio during repeated analyses of the same particle. The O : P stoichiometry is calculated as  $[I_{\text{O}}/I_{\text{P}}] \cdot k_{\text{O:P}} \cdot F_{\text{O}}/F_{\text{P}}$ , where  $I_{\text{O}}$  and  $I_{\text{P}}$  are the O and P net counts,  $k_{\text{O:P}}$  is the k-factor, and  $F_{\text{O}}$  and  $F_{\text{P}}$  are absorption correction factors for O and P X-rays in the sample<sup>11</sup>.

## RESULTS AND DISCUSSION

### Electron microscopy

Thin freeze-dried cryosections of the three microalgae species were examined in the TEM, normally in scanning transmission (STEM) mode. Digital dark-field images of these cell types are shown in Fig. 1 (A-D). The cells contained electron-dense intracellular bodies or granules which appeared bright in the dark-field images. The granules varied in number and appearance in the different cell types. Some basic morphological observations are summarised in Table-1. The bodies were numerous in *Chlamydomonas* and *Anabaena* cells, but few in *Chlorella*. Selected area electron diffraction of the granules in the TEM did not reveal any characteristic crystalline structure.

TABLE-1  
SUMMARY OF MORPHOLOGICAL CHARACTERISTICS OF ELECTRON-DENSE  
GRANULES IN ALGAL CELL CRYOSECTIONS

Dimensions are expressed as length  $\times$  width (in  $\mu\text{m}$ )

	<i>Chlamydomonas</i>	<i>Chlorella</i>	<i>Anabaena</i>
Mean size of cell section profile ( $\mu\text{m}$ )	$8.3 \times 4.1$	$3.4 \times 2.2$	$3.7 \times 2.2$
Number of profiles measured	5	24	21
Mean number of granules per cell section	8.6	1.3	4.0
Mean size of largest granule in a cell section ( $\mu\text{m}$ )	$0.77 \times 0.45$	$0.64 \times 0.39$	$0.56 \times 0.47$
Largest granule observed ( $\mu\text{m}$ )	$1.48 \times 0.71$	$0.93 \times 0.64$	$0.81 \times 0.70$

In *Chlamydomonas*, the granules were irregular in shape, and were associated with cell vacuoles (Fig. 1A), commonly developing from central or peripheral cytoplasm. Those in *Chlorella* were generally large relative to the size of the cell,

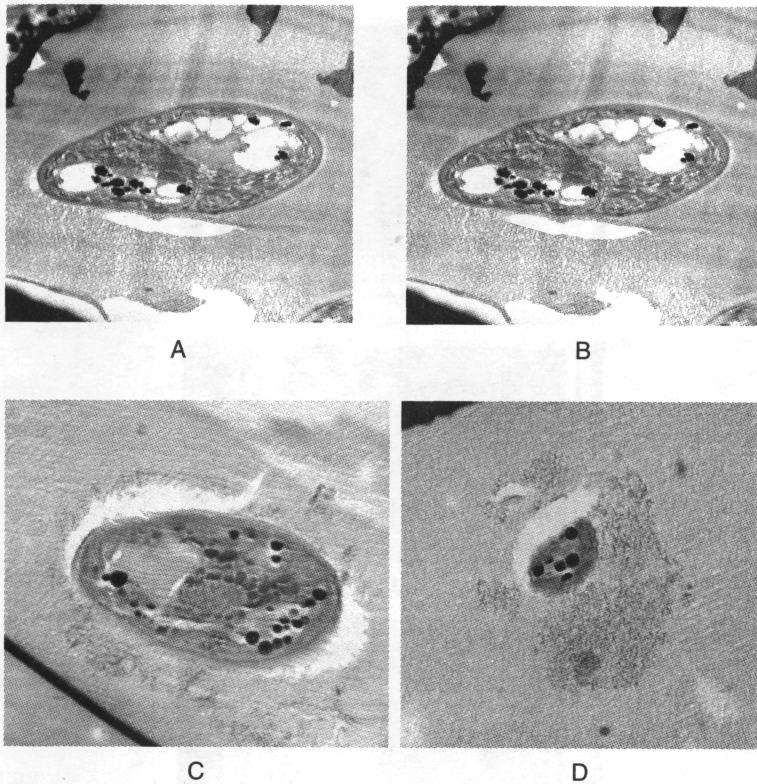


Fig. 1. Electron microscopy analysis of thin sections of (A) *Chlamydomonas reinhardtii*, (B) *Chlorella vulgaris*, (C) *Anabaena circinalis*, and (D) *Anabaena circinalis* cell wall mucilage.

and located in the cytoplasm near the parietal chloroplast (Fig. 1B). In *Anabaena*, the granules were also distributed in the cytoplasm (Fig. 1C). In addition, electron-dense material was frequently observed external to *Anabaena* cells near the cell wall and in the surrounding agarose-albumin matrix from the dried suspension medium (Figs. 1C and 1D). This material presumably corresponds to the gelatinous sheath which characteristically envelops blue-green algae, and which is largely preserved in the cryosections from fresh cell suspensions.

### X-ray microanalysis

X-ray microanalyses of cellular compartments, as well as digital X-ray mapping of whole cell sections, showed that most of the manganese accumulated within the cells was located in the intracellular electron-dense granules. X-ray spectra recorded from a granule as well as from the cytoplasm and cell wall are compared in Fig. 2 for *Chlamydomonas* and in Fig. 3 for *Chlorella*. Spectra from *Anabaena*, obtained from a granule and from the cell wall in contact with the external mucilaginous layer in Fig. 1C, and from a dense region of the gelatinous sheath in Fig. 1D, respectively, are shown in Fig. 4. In all spectra, the CuL line at 0.93 keV derives from the grid material.

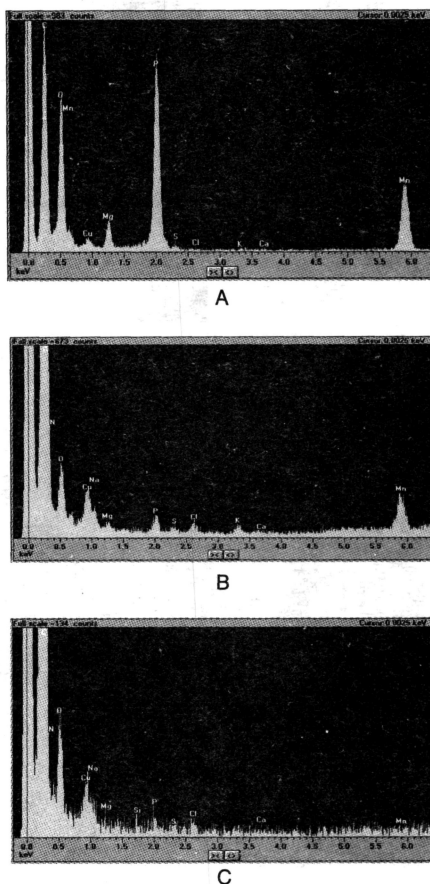


Fig. 2. Representative energy dispersive X-ray analysis of (A) granule, (B) cytoplasm and (c) cell wall in *Chlamydomonas reinhardtii*.

The element distributions in cryosections of the three cell types are presented in the X-ray digital images in Figs. 5–8, which show a major concentration of the accumulated manganese in the intracellular granules. In the *Anabaena* images, large amounts of manganese are evident in the gelatinous material external to the cells (Figs. 7 and 8). Thus, in striking contrast to the chlorophyte algae *Chlamydomonas* and *Chlorella*, in the cyanophyte species *Anabaena* a large proportion of the manganese appeared to be located external to the cells (Fig. 4C and Figs. 7 and 8). Some manganese was also detected in the *Anabaena* cell wall where it was adjacent to the mucilaginous material (Fig. 4B). In both *Chlamydomonas* and *Chlorella*, the manganese was heavily concentrated in the intracellular granules, although small amounts were observed in the cell cytoplasm (Fig. 2B and 3B). No manganese was measured in the cell wall in the two chlorophyte species (Figs. 2C and 3C) at the level of detection for this element (about 500–1000 ppm), nor was it detected in the supporting agarose-albumin matrix of the suspension medium.

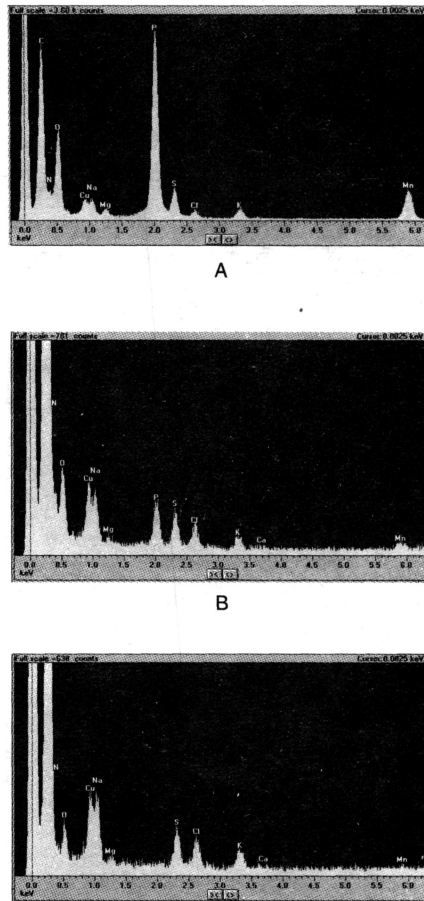


Fig. 3. Representative energy dispersive X-ray analysis of (A) granule, (B) cytoplasm and (C) cell wall in *Chlorella vulgaris*.

The element concentrations (in weight %, on a dry weight basis) that were found in the granules, cytoplasm and cell wall are compared in Figs. 9–11, for each of the three species. The values depicted are those weight concentrations determined within each of the compartments. Thus, for example, the granules contained proportionately much higher weight fractions of O and P than did the cytoplasm or cell wall.

The main elements associated with Mn in the granules were O, P and Mg and in *Chlorella*, also Na, S, Cl and K. Nitrogen was detected in granules from *Chlorella* and *Anabaena* and calcium was present in significant amounts in *Anabaena* granules. Table-2 summarises the results from quantitative analyses of intracellular granules. *Chlamydomonas* granules contained the highest Mn concentrations, in excess of 10% by weight. One such intracellular granule, not included in these results, was found to contain almost pure  $\text{MnO}_2$ .

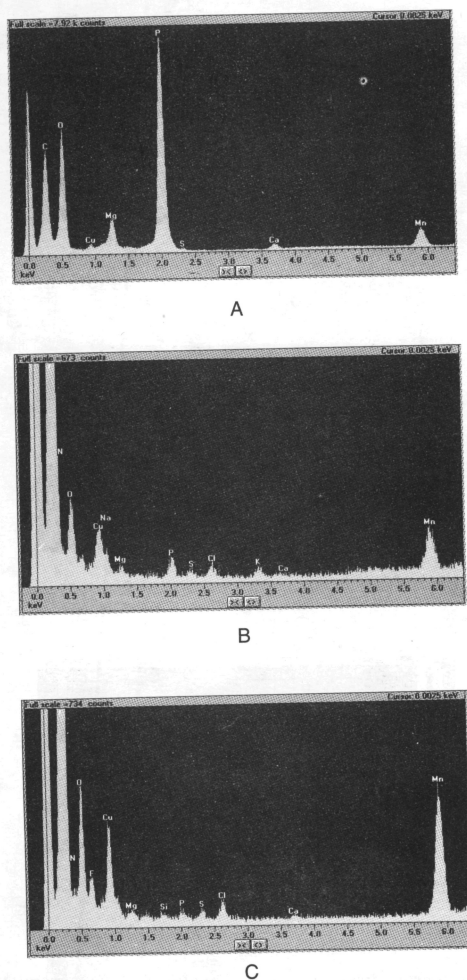


Fig. 4. Representative energy dispersive X-ray analysis of (A) granule, (B) cytoplasm and (C) cell wall in *Anabaena circinalis*.

In the *Anabaena* preparation, high concentrations of Mn were measured in the mucilaginous layer external to the cells. In a dense area of the gelatinous sheath in Fig. 1D, the Mn concentration was as high as 33% by weight. *Chlorella* cells did not exhibit any external mucilage, but some electron-dense bodies observed in the agarose-albumin matrix outside the cells were found to contain, in addition to the elements normally observed in the intracellular granules, high concentrations of Fe, up to 34% by weight (Figure 12).

To investigate the possible chemical forms of phosphorus in the intracellular granules, the oxygen to phosphorus (O:P) stoichiometry in the granules was calculated from the ratios of net intensities of these elements in the X-ray spectra. These results are summarised in Table-3. The uncorrected value represents the minimum ratio before correction for absorption of oxygen and phosphorus X-rays



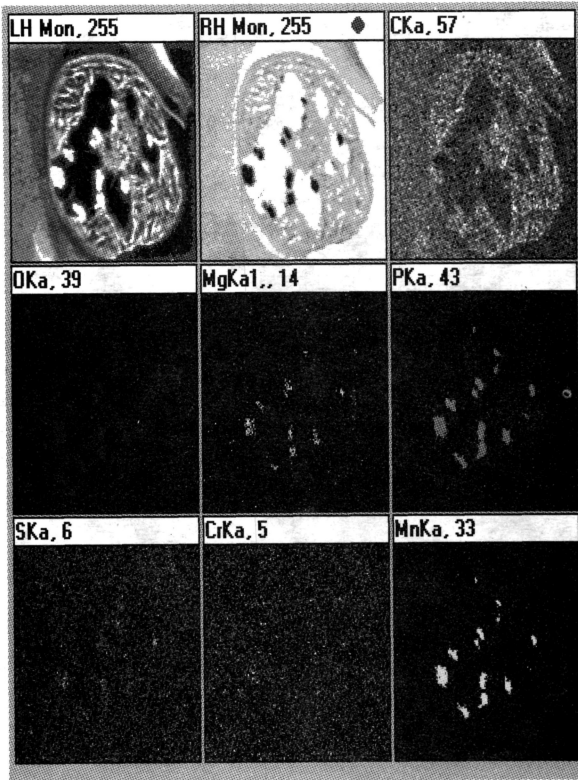


Fig. 5. X-ray map image for *Chlamydomonas reinhardtii* microalgae cell after manganese accumulation

TABLE-2  
ELEMENTAL CONCENTRATION OF MICROALGAE CELL GRANULES IN Wt. %<sup>a</sup>

Specimen	C	N	O	Na	Mg	P	S	Cl	K	Ca	Mn
<i>Chlamydomonas</i> (5 cells, 7 granules)											
	24.41	0.0	37.51	0.23	3.24	23.43	0.29	0.04	0.09	0.07	10.46
	±3.76	±0.0	±3.18	±0.15	±0.3	±1.47	±0.08	±0.04	±0.06	±0.05	±1.74
<i>Chlamydomonmas</i> (at low temperature) (4 cells, 5 granules)											
	20.82	0.0	44.88	0.52	2.84	20.36	0.38	0.1	0.34	0.08	9.62
	±3.45	±0.0	±2.48	±0.26	±1.02	±1.7	±0.19	±0.06	±0.1	±0.05	±1.77
<i>Chlorella</i> (6 cells, 8 granules)											
	28.03	9.84	22.8	3.76	1.2	23.43	4.49	1.3	1.6	0.0	3.48
	±3.01	±1.85	±1.81	±1.37	±0.32	±1.49	±0.47	±0.27	±0.37	±0.0	±0.74
<i>Anabena</i> (7 cells, 10 granules)											
	33.38	5.59	32.22	0.0	2.73	21.32	0.83	0.25	0.50	0.93	1.89
	±5.54	±1.78	±3.33	±0.0	±0.4	±2.44	±0.17	±0.18	±0.17	±0.12	±0.53

Results are means ± SEM.

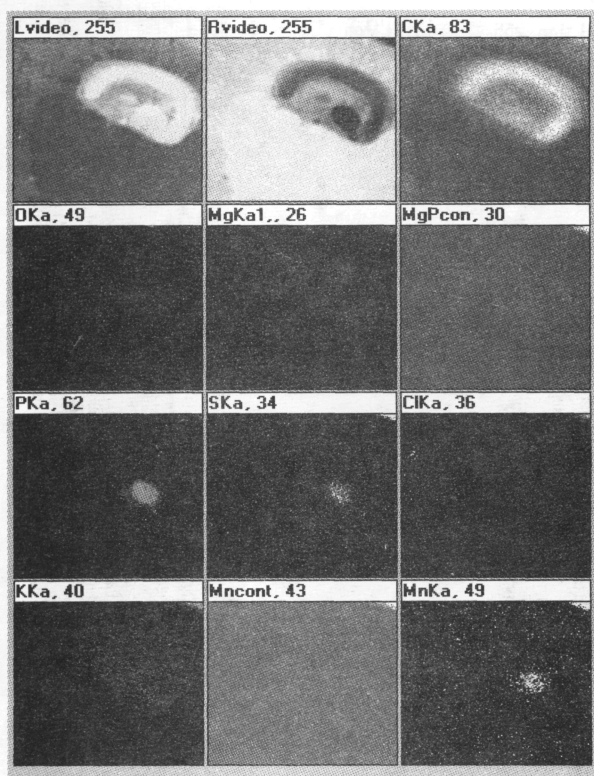


Fig. 6. X-ray map image for *Chlorella vulgaris* cell after manganese accumulation.

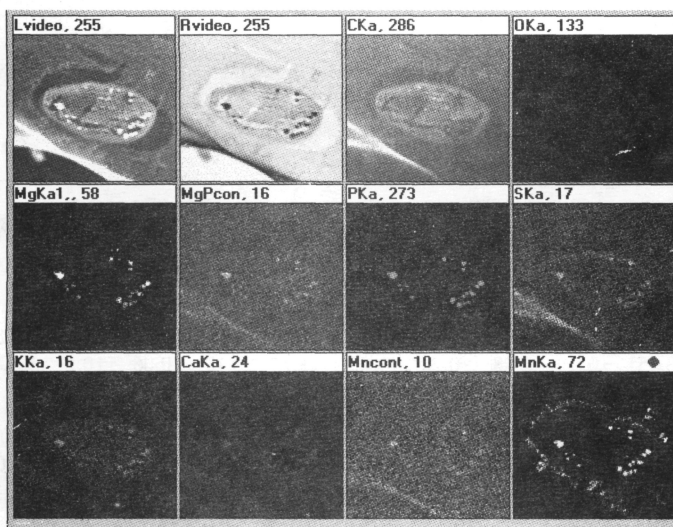


Fig. 7. X-ray map image for *Anabaena circinalis* microalgae cell after manganese accumulation.

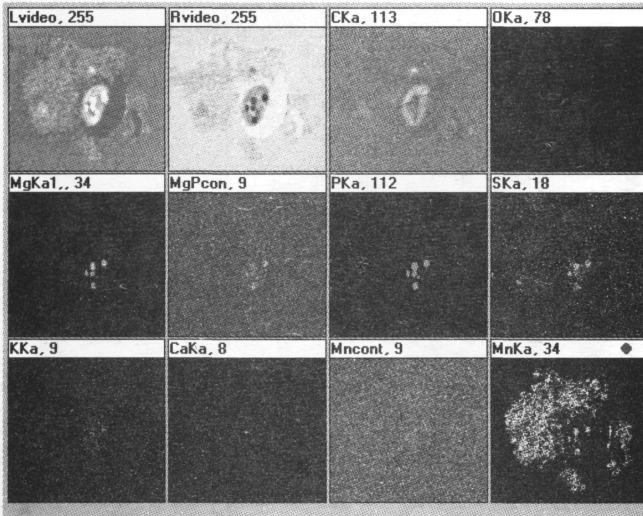


Fig. 8. X-ray map image of the cell wall mucilage of *Anabaena circinalis* cell after manganese accumulation.

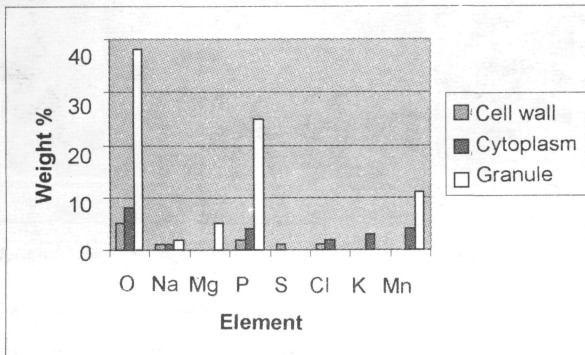


Fig. 9. The elemental concentration (in weight %) that were found in the granules, cytoplasm and the cell wall of *Chlamydomonas reinhardtii*.

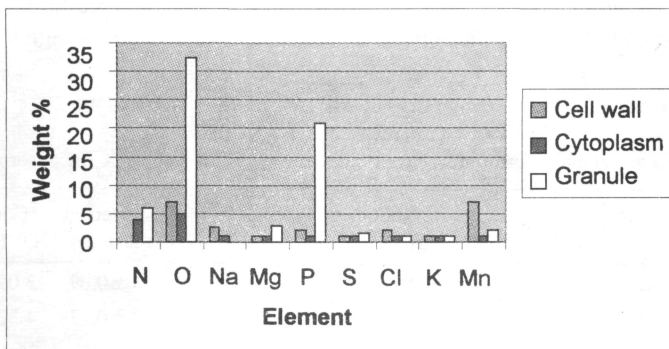


Fig. 10. The elemental concentration (in weight %) that were found in the granules, cytoplasm and the cell wall of *Chlorella vulgaris*.

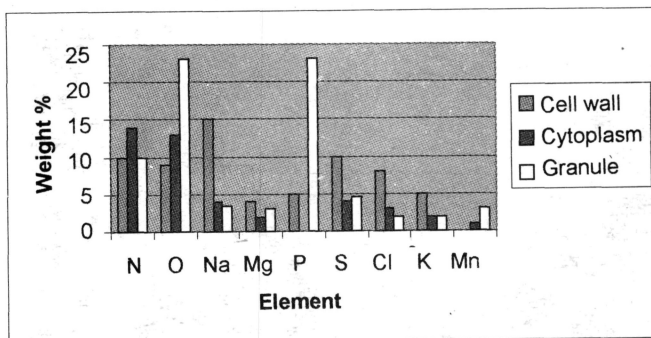


Fig. 11. The elemental concentration (in weight %) that were found in the granules, cytoplasm and the cell wall of *Anabaena circinalis*.

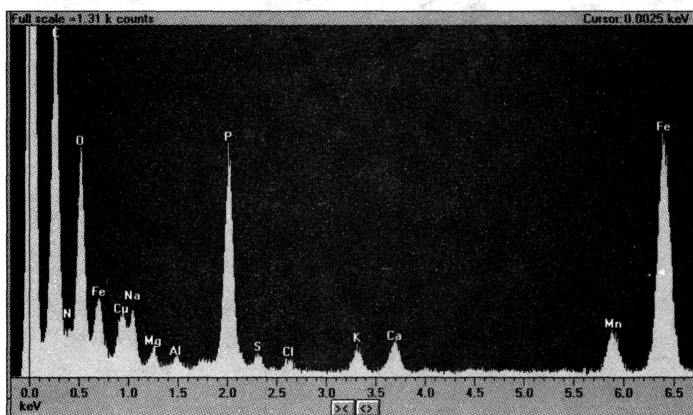


Fig. 12. Representative energy dispersive X-ray analysis of the cell wall mucilage of *Chlorella vulgaris*.

in the sample. The O:P stoichiometry was lowest in *Chlorella* granules, and generally  $> 3$  in *Chlamydomonas* and *Anabaena*. To check whether these values may be underestimated because of differential element loss under the electron beam, some *Chlamydomonas* cells were analysed at low temperature ( $-160^{\circ}\text{C}$ ) to minimise mass loss. The proportions of O and S were somewhat higher in these

TABLE-3  
CALCULATED O : P STOICHIOMETRY IN ELECTRON-DENSE  
INTRACELLULAR GRANULES

The ratio are given before (uncorrected) and correction for sample X-ray absorption

Specimen	No. of cells	No. of granules	Ratio of O to P counts	Uncorrected O : P stoich.	Corrected O : P stoich.
<i>Chlamydomonas</i>	3	7	$0.50 \pm 0.02$	$2.54 \pm 0.09$	$3.09 \pm 0.12$
<i>Chlamydomonas</i> (low temperature)	4	5	$0.73 \pm 0.04$	$3.70 \pm 0.22$	$4.32 \pm 0.21$
<i>Chlorella</i>	6	8	$0.28 \pm 0.02$	$1.41 \pm 0.09$	$1.9 \pm 0.11$
<i>Anabena</i>	7	10	$0.47 \pm 0.05$	$2.42 \pm 0.25$	$3.12 \pm 0.30$

granules than for those analysed at room temperature (Table-2). The time-course of possible mass loss was checked by repeatedly analysing the same granule for short periods. Figs. 13 and 14 show the change in the ratios of elemental counts

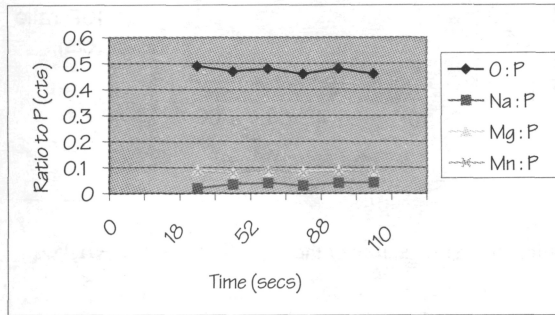


Fig. 13. The time-course of potential mass loss of element count to phosphorus for *Chlamydomonas* cell (3 granule) at room temperature.

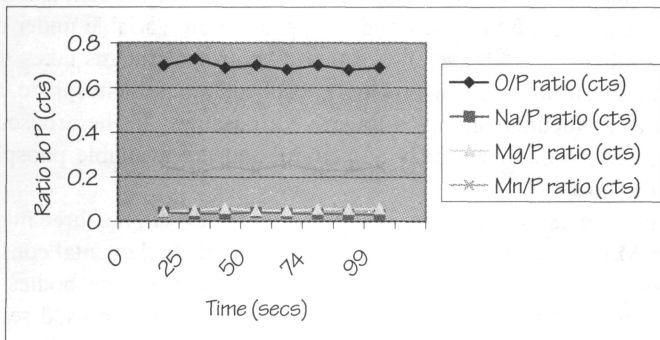


Fig. 14. The time-course of potential mass loss of element counts to phosphorus for *Chlamydomonas* cell (3 granule) at low temperature ( $-160^{\circ}\text{C}$ ).

to phosphorus in two *Chlamydomonas* granules at room temperature and low temperature, respectively. The O/P ratio exhibited a small decline at room temperature, which was virtually abolished at low temperature. The ratios of the other main elements in the granules did not change markedly. For comparison, the stability of the phosphate group in  $\text{KH}_2\text{PO}_4$  was checked by sequential analyses of a small particle of the salt (Fig. 15). Although the potassium decreased with time during analysis at room temperature, the O/P ratio remained stable.

Various microorganisms, including algae, have been reported to contain condensed phosphate entities<sup>12-14</sup> generally consisting of varying chain length; storage of these phosphate polymers is often via cytoplasmic inclusion<sup>15, 16</sup>. In addition, it is well established that some microorganisms are capable of synthesizing inorganic polyphosphate<sup>17, 18</sup>. The proposed functions of such polyphosphate are as energy storage polymers<sup>19</sup>, regulation of the cellular orthophosphate levels<sup>20</sup>, and as regulators of metabolic processes, through control of the

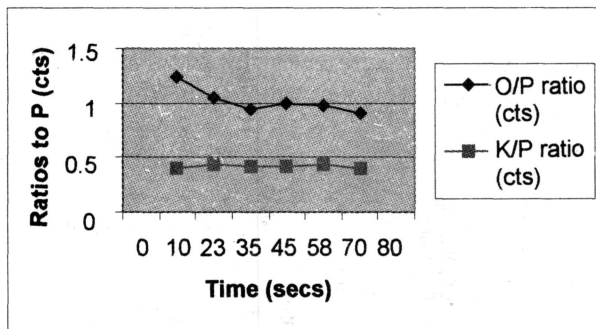


Fig. 15. The stability of the phosphate group in  $\text{KH}_2\text{PO}_4$ .

biosynthesis of nucleic acids and phospholipids under conditions of phosphorus starvation<sup>21</sup>. In addition, phosphate has been proposed to act as a control factor in cell division in *Chlamydomonas reinhardtii*<sup>22</sup>. Jensen and Sicko<sup>23</sup> have shown that polyphosphate bodies can develop in different areas of the cell; and the mode of formation and structure of such bodies appears quite variable under different conditions. Callow *et al.*<sup>24</sup> have shown that mycorrhizal fungus takes up phosphate from the environment, converts this phosphate into polyphosphate, and then translocates it as vacuolar granules to active arbuscules. In the arbuscules, the granules are broken down by enzyme activity and the available phosphorus is released to the host.

In this study we have shown that polyphosphate bodies in the three microalgae cells contain Mn, Mg, and S in addition to P as their major elemental constituents; calcium was not found as a constituent of the polyphosphate bodies in both *Chlamydomonas* and *Chlorella*. A number of researchers have used sections of fixed and embedded biological specimens analyzed by means of X-ray energy dispersive systems in order to determine the major elemental constituents of polyphosphate bodies. Sicko-Goad *et al.*<sup>25</sup> have reported that, in the blue-green alga *Plectonema boryanum*, calcium was a major component of the polyphosphate bodies, but the exact role of calcium in the metabolism of phosphorus bodies has yet to be determined; they suggested that the consistency in the occurrence of the phosphorus-calcium association suggests a relationship that is more than fortuitous. Hutchinson *et al.*<sup>26</sup> used zoopore  $\gamma$  particles of *Blastocliadiella emersonii* to find the composition of these bodies, and found that some particles contained P, K and Ca, others lacked K but contained P and Ca, while still others contained K, S, and Cl. Jones and Chambers<sup>27</sup> isolated polyphosphate bodies from *Desulfovibrio gigas* and found Mg, P, and organic carbon compounds. Thus, it appears from previous studies that the composition of polyphosphate bodies may be associated with P, K, Ca, Mg, S and Cl and an organic component; how the different components of the polyphosphate bodies function in overall cell metabolism in microorganisms is not adequately known.

The O:P stoichiometric ratios are the only ones so treated here, as we were interested in obtaining information concerning the nature of the phosphorus present inside the cells in the granules. Such phosphorus could be present as simple

phosphate O:P = 4:1), long chain polymeric polyphosphate (O:P = 3:1), or two-dimensional polymeric polyphosphate (O:P = 2:1), as well as various organic phosphates. It is not possible from the median results for either *Chlamydomonas* or *Anabena* to make conclusions about the nature of the phosphate; however the results for *Chlorella* clearly indicate a very low O:P ratio of approx. 2:1; this would appear only to be achievable (assuming that the oxidation state of P is +5) in a two-dimensional polymeric polyphosphate system.

It is presumed that the chemical structure of the polyphosphate bodies offers convenient sites for the binding of manganese via a process of metabolic reaction to remove high concentration of manganese ions from the cytoplasm. Indeed, our results suggest that these bodies are important in maintaining low concentrations of free metal ions within the cells and thus reducing any metal toxic effect. This approach offers an explanation for the resistance mechanism in microorganisms. It may be the case that the microalgae cells originally have polyphosphate bodies in which the available binding sites are already occupied by magnesium; after exposure to manganese, isomorphous replacement of magnesium takes place to bind the polyphosphate binding sites.

Magnesium plays many key intracellular roles, including activating many enzymes and stabilizing ribosomes<sup>28</sup>, Thilo<sup>29,30</sup> has noted that  $Mg^{2+}$  is an important catalyst in the degradation of polyphosphate polymers. Our results suggest that manganese is a competitive inhibitor in the magnesium metabolism system, which causes loss of magnesium from its binding sites. Indeed, manganese is known to replace magnesium in a variety of biological functions, amongst them the  $Mg^{2+}$ -ATP activated uptake of catecholamines into isolated granules<sup>31</sup>. Silver *et al.*<sup>32</sup> have shown that when manganese enters inside the bacterial cells of *Escherichia coli*, it displaces the internal magnesium and leads to a net cellular loss and hence growth inhibition.

Our results have shown the association of manganese with sulfur in the granules in *Chlorella*. Sulfur has been implicated in metal tolerance mechanisms in a number of microorganisms which live in an environment containing high concentrations of metal ions. Manganese associated with sulfur may be either in an inorganic form (sulphide, sulphite, etc.) or complexed with protein (metallothionines), rich in sulfur-containing residues (cysteine, cystine, methionine). The occurrence of protein inside the granules is not an unexpected result, as phosphorus-rich inclusions have been reported to contain protein, DNA, RNA and lipid<sup>33</sup>.

Ghandour *et al.*<sup>34</sup> studied the ability to accumulate silver of growing and non-growing cultures of *E. coli* cells isolated from sludge. They found that growing bacteria accumulated silver both on the surface and via intracellular uptake.

Ashida<sup>35</sup> has found that a copper-tolerant yeast has precipitated excess copper extracellularly as sulphide (cupric sulphide), Ashworth and Amin<sup>36</sup> have found that mercury tolerance in *Aspergillus niger* was due to a pool of nonprotein sulphhydryl groups, while Walker and Brown<sup>38</sup> have shown that sulfur is important in the development of copper granules in the barnacle *Balanus balanoides* and in the isopod *Asellus*.

Very recently Mattuschka *et al.*<sup>39</sup> have studied the resistance of the bacterial cells *Pseudomonas stutzeri* and *Streptomyces albus* to the metal ions silver, copper, lead and zinc, while Salwson *et al.*<sup>40-42</sup> have studied silver resistance to the bacterial cells *Pseudomonas stutzeri* and have mentioned the involvement of sulfur in the resistance mechanism.

Our results have shown that manganese ions complex with electron donor groups containing oxygen, phosphorus, sulphur and nitrogen in the external mucilage of *Anabena*. In biological systems, these elements are normally present as phosphates, thiols, hydroxyl amines, and indoles<sup>43</sup>. Thus our proposal is that manganese was accumulated by an energy-independent process and ultimately bound at specific sites within the cell. Once these specific sites become saturated, absorption inside the cell wall occurs. Therefore, manganese biosorption by the microorganism is a phenomenon occurring in two stages: a rapid, reversible and metabolic independent surface binding of manganese to reactive groups within the cell wall, followed by nucleation of the deposition of more metal at the same location, and then metabolic dependent irreversible intracellular accumulation of manganese inside the cell.

From a biotechnology perspective, the idea of using microorganism strains to recover manganese from effluents or in mining operations involves consideration of many factors. For example, when the living cells accumulate large amounts of the metal inside the cell, the metal is not eluted from the cells which thereby die. Therefore, living microalgal strains may not be of any great biotechnological value in manganese recovery.

Some results show the presence of both iron and manganese combined together in the agarose-albumin matrix outside *Chlorella* cells. The iron present could be accumulated from the growth medium before exposure to manganese solution. Co-accumulation of iron and manganese is great. This co-accumulation via algal mediation fits the pattern whereby the two metals are deposited by microorganisms present in environments in lake regions<sup>44</sup>. It should be remembered that iron and manganese have a similar distribution and are found as major or minor components of a large variety of rocks, minerals and ore deposits<sup>45</sup>. Furthermore, being metals required by living systems, both metals are concentrated in biological materials and thus participate in the biological cycle.

## REFERENCES

1. P.M. Stokes, T.C. Hutchinson and K. Krauter, *Can. J. Bot.*, **51**, 2155 (1973).
2. H. Aiking, A. Stijman, C. Van Garderen, H. Van Hearkuizen and R. Vant, *Appl. Environ. Microbiol.*, **47**, 374 (1984).
3. L.E. Macaskie, A.C.R. Dean, A.K. Cheetham, R.J.B. Jakeman and A.J. Skarnulis, *J. Gen. Microbiol.*, **133**, 539 (1987).
4. M.E. Starodub and J.T. Trevors, *J. Med. Microbiol.*, **29**, 101 (1989).
5. C. Haefeli, C. Franklin and K. Hardy, *J. Bacteriol.*, **158**, 389 (1984).
6. R.M. Slawson, H. Lee and J.T. Trevors, *Biol. Met.*, **3**, 151 (1990).
7. R.M. Slawson, M.I. Van Dyke, H. Lee and J.T. Trevors, *Plasmid*, **27**, 72 (1992).
8. R.M. Slawson, J.T. Trevors and H. Lee, *Arch. Microbiol.*, **158**, 398 (1992).
9. R.J. Graham and J.W. Steed, *J. Microscopy*, **133**, 275 (1984).



10. Z. Horita, T. Sano and M. Nemoto, *J. Microscopy*, **143**, 215 (1986).
11. G. Cliff and G.W. Lorimer, *J. Microscopy*, **103**, 203 (1975).
12. H. Tamiya, *Ann. Rev. Plant Physiol.*, **17**, 1 (1966).
13. F.M. Harold, *Biochim. Biophys. Acta*, **45**, 172 (1960).
14. H. Voelz, U. Voelz and R.O. Ortiyoza, *Arch. Mikrobiol.*, **53**, 371 (1966).
15. T.E. Jensen, *Arch. Mikrobiol.*, **62**, 144 (1968).
16. N. Munk and H. Rosenberg, *Biochim. Biophys. Acta*, **177**, 629 (1969).
17. F.M. Harold, *Bacteriol. Rev.*, **30**, 772 (1966).
18. S. Mudd, A. Yoshida and M. Koike, *J. Bacteriol.*, **75**, 224 (1958).
19. S. Mryachi, R. Kanai, S. Mihara, S. Miyachi and S. Aoki, *Biochim. Biophys. Acta*, **93**, 625 (1964).
20. F.M. Harold, *Biochim. Biophys. Acta*, **45**, 172 (1960).
21. I.S. Kulacv, in: *The Biochemistry of Inorganic Polyphosphates*, John Wiley & Sons, Inc., New York (1989).
22. T. Lien and G. Knutsen, *Exp. Cell. Res.*, **78**, 70 (1973).
23. T.E. Jensen and L.M. Sicko, *Can. J. Microbiol.*, **20**, 1235 (1974).
24. J.A. Callow, L.C.M. Capaccio, G. Parish and P.B. Tinker, *New Phytol.*, **80**, 125 (1978).
25. L.M. Sicko-Goad, R.E. Crang and T.E. Jensen, *Cytobiologie Z. Exp. Zellforsch.*, **11**, 430 (1975).
26. T.E. Hutchinson, M.E. Cantino and E.C. Cantino, *Biochem. Biophys. Res. Commun.*, **74**, 336 (1977).
27. H.E. Jones and L.A. Chambers, *J. Gen. Microbiol.*, **89**, 67 (1975).
28. S. Silver and D. Clark, *The Journal of Biological Chemistry*, **246**, 569 (1971).
29. E. Thilo, *Advan. Inorg. Chem. Radiochem.*, **4**, 1 (1962).
30. \_\_\_\_\_, *Colloq. Intern. Centre Natl. Rech. Sci. (Paris)*, **106**, 491 (1962).
31. N. Kirshner, *J. Biol. Chem.*, **237**, 2311 (1962).
32. S. Silver, P. Johseine, E. Whitney and D. Clark, *J. Bacteriol.*, **110**, 186 (1972).
33. I. Friedberg and G. Avigad, *J. Bacteriol.*, **96**, 544 (1968).
34. W. Ghandour, J.A. Hubbard, J. Deistrung, M.N. Hughes and R.K. Poole, *Appl. Microbiol. Biotechnol.*, **28**, 559 (1988).
35. J. Ashida, *Ann. Rev. Phytopathol.*, **3**, 153 (1965).
36. L.T. Ashworth and T.V. Amin, *Phytopathol.*, **54**, 1459 (1964).
37. G. Walker, *Mar. Biol.*, **39**, 343 (1977).
38. B.E. Brown, *Prac. Freshwater Biology*, **7**, 235 (1977).
39. B. Mattuschka, G. Straube and J.T. Trevors, *Biol. Met.*, **7**, 201 (1994).
40. R.M. Slawson, M. Lee and J.T. Trevors, *Biol. Met.*, **3**, 151 (1990).
41. R.M. Slawson, M.I. Van Dyke, H. Lee and J.T. Trevors, *Plasmid*, **27**, 72 (1992).
42. R.M. Slawson, J.T. Trevors, and H. Lee, *Arch. Microbiol.*, **158**, 398 (1992).
43. S.S. Block Edition, in: *Disinfection, Sterilization and Preservation*, 2nd edn., Lea and Febiger, Philadelphia (1977).
44. K.H. Nealsop, in: N.D. Holland and K.S.V. Schidlows (eds.), *Mineral Deposits and the Evolution of the Biosorption*, Berlin, p. 51 (1982).
45. H. Lepp, in *Geochemistry of Iron*, John Wiley and Sons, Inc. (1985).